Strong effect of substrate termination on Rashba spin-orbit splitting: Bi on $BaTiO_3$(001) from first principles

Samir Abdelouahed* and J. Henk
Max-Planck-Institut für Mikrostrukturphysik, Weinberg 2, Halle, D-06120 Saale, Germany
(Received 21 September 2010; published 29 November 2010)

We demonstrate by first-principles calculations that the Rashba spin-orbit splitting in the 6*p* states of a Bi adlayer on $BaTiO_3$(001) is strongly affected by the substrate termination. For the TiO_2 termination the absolute splitting is very large (about 0.23 Å^{-1}); in contrast, the splitting becomes strongly reduced for the BaO termination (less than 0.07 Å^{-1}). Our findings are explained by the termination-dependent hybridization of the Bi surface states with electronic states in the substrate.

DOI: 10.1103/PhysRevB.82.193411 PACS number(s): 73.20.At, 77.84.Ek, 77.84.Cg, 71.70.Ej

I. INTRODUCTION

The Rashba effect[1] has become a notable topic in condensed-matter physics. It is not only important with respect to spintronic applications[2–5] but also allows to study in detail spin-orbit effects in the surface states of metals [e.g., Au(111) (Refs. 6 and 7)] and in surface alloys [e.g., Bi/Ag(111) (Ref. 8)]. Already for the *L*-gap surface states at the (111) surfaces of noble metals (Cu, Ag, and Au) (Ref. 9) the importance of the atomic spin-orbit coupling has been proven.[10] For the surface alloys—build by adlayers of Bi, Pb, and Sb on Ag(111) and Cu(111)—further mechanisms which influence the strength of the Rashba splitting have been identified. To name two, the relaxation and the strength of the atomic spin-orbit coupling in the adlayer.[11–16]

With respect to tuning the Rashba characteristics, that are the splitting k_R and the Rashba energy E_R, we have recently proposed a so far unexplored type of system:[17] a monolayer of Bi on $BaTiO_3$. In a first-principles investigation we showed that the Bi 6*p* states exhibit a large spin splitting ($k_R \approx 0.23$ Å^{-1}). Further, reversing the electric polarization *P* in the ferroelectric $BaTiO_3$ substrate changes the Rashba characteristics by about 5%. In that study the substrate was terminated by a TiO_2 layer.

In view of the large spin splitting in Bi/Ag(111) (and similar systems) and in Bi/$BaTiO_3$, one could conclude that any heavy-element adlayer on a surface displays a large Rashba effect. In this Brief Report we show that this conjecture does not hold: by changing the TiO_2 termination to BaO termination, the Rashba splitting of the Bi surface states becomes strongly reduced by about 1 order of magnitude ($k_R \approx 0.03$ Å^{-1}). To our knowledge, such strong an effect of the substrate[14] on the Rashba splitting has not been reported so far.

Our findings force us to address in detail the mechanisms which determine the strength of the Rashba effect in detail. We will show that hybridization of the Bi states with those of the substrate plays a decisive role. Here, the charge-density profile becomes equivalent to a potential gradient via the Poisson equation. This effective potential gradient leads to an asymmetry of the surface-state wave function close to the Bi atoms, that is, where the atomic spin-orbit coupling is strongest. As a consequence, the spin splitting becomes sizable. Further, the image-potential barrier at the surface barrier is irrelevant here.

II. RASHBA EFFECT

The Rashba effect is simply modeled by an isotropic two-dimensional electron gas. The dispersion relations of the free electrons which are confined to the *xy* plane read[18]

$$E_{\pm}(\vec{k}_{\parallel}) = \frac{\hbar^2 \vec{k}_{\parallel}^2}{2m^*} \pm \gamma_R |\vec{k}_{\parallel}| + E_0, \quad \vec{k}_{\parallel} = (k_x, k_y), \tag{1}$$

where the split electronic states are labeled by + and −. $m^\star$ is the effective electron mass. The Rashba parameter γ_R quantifies the spin-orbit coupling strength and comprises effectively two contributions.[10] The "atomic" contribution is due to the strong potential of the ions and the "confinement" contribution is due to the gradient of the confinement potential in *z* direction. The Rashba characteristics can be read off the dispersion relation, Eq. (1). The splitting

$$k_R = \frac{|m^*|\gamma_R}{\hbar^2} \tag{2}$$

is defined as the shift of the band extremum off the Brillouin-zone center ($\vec{k}_{\parallel}=0$) and the Rashba energy

$$E_R = -\frac{\hbar^2 k_R^2}{2m^*} = -\frac{m^* \gamma_R^2}{2\hbar^2} \tag{3}$$

is the energy of the band extremum with respect to the energy E_0 at which the bands cross. Since Kramers' degeneracy is lifted, the electronic states are completely spin polarized. Their spin polarizations are within the *xy* plane and are normal to $\vec{k}_{\parallel}$. Further, the spins of the split states are oppositely oriented.

III. COMPUTATIONAL ASPECTS

Our *ab initio* approach relies on the local-density approximation to density-functional theory, as formulated in the full-potential linearized augmented plane-wave (FLAPW) method.[19] The computations have been performed using the FLEUR code.[20] The surface system is mimicked by a slab which consists of six layers of $BaTiO_3$ and a Bi adlayer. The experimental in-plane lattice constant of $a=7.53a_0$ with $c/a=1.011$ (Ref. 21) is used. The muffin-tin radii R_{mt} are set to $3.0a_0$ for both Bi and Ba, $2.18a_0$ for Ti, and $1.39a_0$ for O.

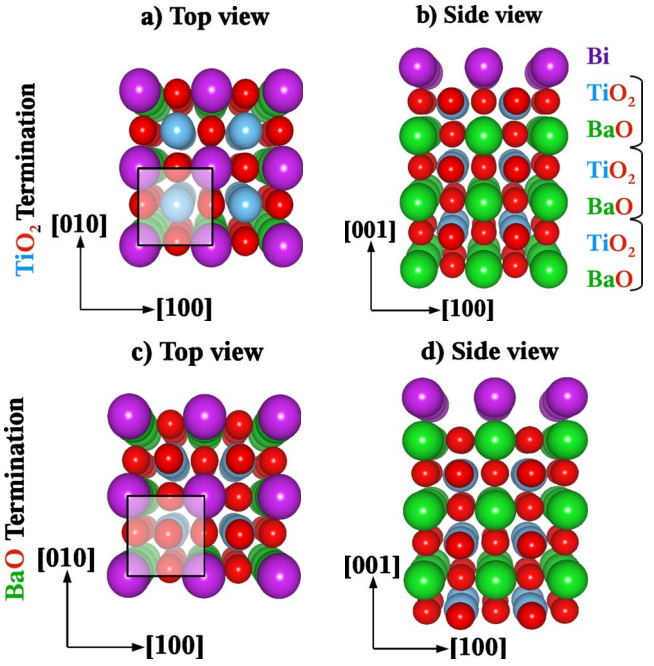

FIG. 1. (Color online) Perspective view of the surface geometries of Bi/$BaTiO_3$(001) with TiO_2 termination (top row) and BaO termination (bottom row). The left (right) column shows a top (side) view. The atomic species are indicated by color and size of the spheres (Bi: violet, large; Ba: green large; Ti: blue, medium sized; and O: red, small); confer legend in panel (b).

The plane-wave cutoff for the basis functions is set to $K_{max}=4.7a_0^{-1}$.

We consider $BaTiO_3$ substrates with either TiO_2 or BaO termination. The electric polarization $\vec{P}$ is due to the mutual displacement of the Ti and O atoms (Ba and O atoms) in each layer. It is thus along the surface normal and either oriented toward the surface ($P_\uparrow, P>0$) or toward the bulk ($P_\downarrow, P<0$).[22,23] We note that for both TiO_2 and BaO terminations, the polarization in the top most layer is negative, irrespective of the bulk polarization.

In each case, the Bi adatoms form a 1×1 monolayer. For the TiO_2 termination, Bi resides in a hollow site of the (001) surface [Figs. 1(a) and 1(b)] while for the BaO termination, Bi sits on top of Ba [Figs. 1(c) and 1(d)]. The geometries have been relaxed to their equilibrium. Details of the surface geometry are summed up in Table I.

IV. RESULTS AND DISCUSSION

The first-principles calculations were performed in three steps. First, we used the experimental geometry of bulk $BaTiO_3$ (Ref. 21) to simulate the unrelaxed $BaTiO_3$ slab ("unrelaxed $BaTiO_3$" in Table I). Then, we consider a clean TiO_2 and BaO-terminated $BaTiO_3$(001) substrate with the polarization $\vec{P}$ along the z direction ($P_\uparrow$) and the $-z$ direction ($P_\downarrow$). The topmost layers of the slab are relaxed to equilibrium: two TiO_2 layers and one BaO layer for TiO_2-terminated $BaTiO_3$ [Fig. 1(b)] and two BaO layers and one TiO_2 layer for BaO-terminated $BaTiO_3$ [Fig. 1(d)]. Only Ti and O positions were relaxed while the Ba positions were kept fixed.

TABLE I. Geometries of Bi on TiO_2- and BaO-terminated $BaTiO_3$(001). The z distances δ along the [001] direction of $BaTiO_3$ stacks of the subsubsurface (S-2), the subsurface (S-1), and the surface (S) are given for bulk electric polarization $P_\uparrow$ (top) and $P_\downarrow$ (bottom) for both TiO_2- and BaO-terminated slabs.

δ (Å)		Unrelaxed $BaTiO_3$		Relaxed $BaTiO_3$	
Termination		TiO_2	BaO	TiO_2	BaO
$P_\uparrow$	S	0.089	0.073	−0.086	−0.020
	S-1	0.073	0.089	0.110	0.036
	S-2	0.089	0.073	−0.040	0.031
$P_\downarrow$	S	−0.089	−0.073	−0.117	−0.044
	S-1	−0.073	−0.089	−0.050	0.013
	S-2	−0.089	−0.073	−0.060	−0.005

Table I displays the z distances δ between Ti and O atoms of the topmost $BaTiO_3$ layers (S, S-1, and S-2). δ is defined as $\delta\equiv z_{Ti}-z_O$ for TiO_2 and $\delta\equiv z_{Ba}-z_O$ for BaO layers, respectively. For $\vec{P}$ along the z ($-z$) direction ($P_\uparrow$), we have $\delta>0$ ($\delta<0$).

Even when the polarization is $P_\uparrow$ in unrelaxed $BaTiO_3$ ($\delta>0$, TiO_2 termination), O atoms are more relaxed outward than Ti atoms ($\delta<0$), and the polarization reverses in the topmost layer after relaxation, in agreement with earlier computational results.[22] Furthermore, this hold for the BaO-terminated $BaTiO_3$ as well. One might speculate whether this observation is common to many oxide surfaces, irrespective of their bulk geometry.

Now we turn to the Rashba spin-orbit effect in the Bi adlayer. Using the Korringa-Kohn-Rostoker (KKR) method,[24,25] we have recently shown that TiO_2-terminated $BaTiO_3$ induces a Rashba splitting k_R of about 0.23 $Å^{-1}$ in the Bi $6p$ states (Ref. 17). These states lie in the fundamental band gap of $BaTiO_3$. Our KKR results are fully reproduced by the present FLAPW calculations. More precisely, the surface states in the Bi adlayer exhibit a Rashba splitting of up to 0.27 $Å^{-1}$ for TiO_2-terminated $BaTiO_3$ (Fig. 2). The striking observation is that the spin splitting is strongly reduced to less than 0.07 $Å^{-1}$ for BaO-terminated $BaTiO_3$ (central inset in Fig. 2). We note that the dispersion displayed in Fig. 2 does not change qualitatively for the relaxed structures and for opposite polarization P.

In order to disentangle the crucial difference between the TiO_2 and the BaO termination with regard to the Rashba splitting we address the charge density at the Bi/$BaTiO_3$ interface. Figure 3 presents two-dimensional charge densities in the energy interval of the Bi $6p$ valence states. For the TiO_2 termination [Fig. 2(b)], we find that the Bi $6p$ surface states hybridize strongly with Ti states in the topmost substrate layer. The charge density is pronouncedly elongated in lateral direction. A similar bonding has been found for a

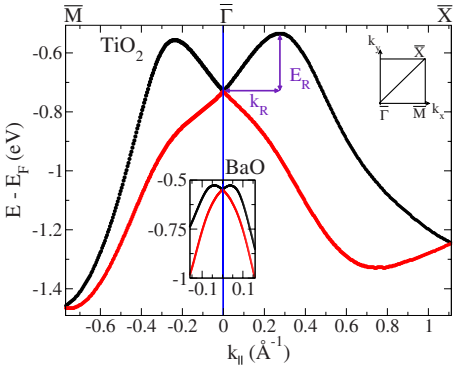

FIG. 2. (Color online) Rashba splitting of Bi 6*p* surface states in $Bi/BaTiO_3(001)$. The main panel displays the dispersion of the surface states for TiO_2-terminated $BaTiO_3$ (unrelaxed, $P_\downarrow$) along the high-symmetry lines of the two-dimensional Brillouin zone (inset). The dispersion close to $\bar{\Gamma}$ ($\vec{k}_\parallel=0$) for BaO-terminated $BaTiO_3$ is depicted in the central inset (with the same $k_\parallel$ scale as in the main panel). Note the strongly reduced Rashba splitting k_R in the latter case.

monolayer of Fe on $BaTiO_3$.[23] For the BaO termination [Fig. 2(d)], the charge density is aligned in the direction normal to the surface. Furthermore, it is mostly spherical in the vicinity of the Bi atoms and, thus, indicates weak hybridization with Ba states.

The Rashba effect requires a breaking of the inversion symmetry which is naturally the case at a surface. The strength of the effect is mainly determined by—besides a strong atomic spin-orbit coupling (atomic contribution) (Ref. 13)—a potential gradient normal to the surface (confinement contribution). In a first picture, this potential gradient is due to the image-potential barrier. Since the slope of the image-charge potential is similar for the TiO_2 and the BaO termination, it cannot explain the reduction in the spin splitting by about 1 order of magnitude. Therefore, the wave function of the Bi surface state has to be affected by the $BaTiO_3$ termination in a region where the atomic spin-orbit coupling is strong, that is, close to the Bi position. To elucidate this picture in more detail we show the charge density at cuts through the Bi atoms. Figures 3(a) and 3(c) show clearly that the 6*p* charge density of Bi is asymmetric around the Bi position for the TiO_2 termination [Fig. 3(a)]. In contrast, it is mostly symmetric for the BaO termination [Fig. 3(c)].

These findings suggest that the strong reduction in the Rashba splitting with $BaTiO_3$ termination is mediated by the hybridization with electronic states at the subsurface layers. For TiO_2 termination, the sizable hybridization leads to an imbalance (asymmetry) of the charge density at the Bi position (where the atomic spin-orbit interaction is strongest). Via the Poisson equation, this is equivalent to a potential gradient normal to the surface which eventually results in a large spin splitting. For the BaO termination, the small hybridization leads to a mostly symmetric charge density at the Bi atoms and, consequently, the spin splitting is much less than in the former case. We note in passing that the strength of the effective potential gradient could also be influenced by the atomic potentials: for the TiO_2 termination the hybridization is among the heavy Bi atoms ($Z_{Bi}=83$) and the light Ti

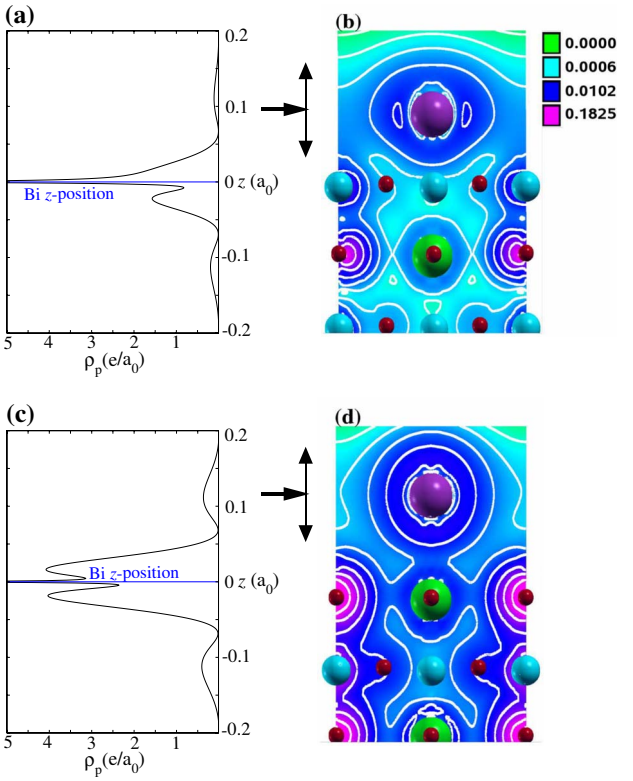

FIG. 3. (Color online) Charge density at the $Bi/BaTiO_3(001)$ surface for TiO_2 termination (top row) and BaO termination (bottom row). Panels (b) and (d) on the right-hand side display the charge density in an energy window that contains the Bi 6*p* states as color scale [increasing from green (light gray) to pink (dark gray) in units of e/a_0^2]. The cut is along the (110) plane. Atoms are represented as in Fig. 1. Panels (a) and (c) on the left-hand side show the Bi 6*p* charge density close to the Bi atoms, at a cut along the *z* direction with *x* and *y* at the lateral (*xy*) Bi position. The displayed *z* range is indicated by the vertical arrows between (a) and (b) as well as between (c) and (d).

atoms ($Z_{Ti}=22$) while for BaO termination it among Bi and the moderately heavy Ba atoms ($Z_{Ba}=56$).

The above findings are robust against relaxation and orientation of the electric polarization in the $BaTiO_3$ substrate. Table II summarizes the Rashba characteristics for the two polarizations $P_\uparrow$ and $P_\downarrow$ and for both $BaTiO_3$ terminations (TiO_2 and BaO). Two conclusions can be drawn from this table. First, irrespective of the polarization, the Rashba parameters k_R and E_R are about one order of magnitude larger (from 5 to 10 times) for the TiO_2 termination as compared to the BaO termination. Second, the strength of the Rashba effect is slightly larger for a relaxed $BaTiO_3$ slab than for an unrelaxed $BaTiO_3$ slab. It turns out that the relaxation of the $BaTiO_3$ slab allows for an increased hybridization with the electronic states in the Bi adlayer (cf. Table I).

V. CONCLUSION

Summing up, our first-principles results show that hybridization of electronic states in an adlayer with those in the substrate can be a key condition for a sizable Rashba spin-

TABLE II. Rashba characteristics for $Bi/BaTiO_3(001)$. The splitting k_R and the Rashba energy E_R of the Bi $6p$ surface states are given for TiO_2- and BaO-terminated $BaTiO_3$ as well as for electric polarizations $P_\uparrow$, and $P_\downarrow$. k_R and E_R are extracted from the dispersions, as is indicated in Fig. 2.

			Unrelaxed $BaTiO_3$		Relaxed $BaTiO_3$	
Termination			TiO_2	BaO	TiO_2	BaO
k_R (Å^{-1})	$P_\uparrow$	$\bar{\Gamma}-\bar{M}$	0.20	0.040	0.22	0.030
		$\bar{\Gamma}-\bar{X}$	0.25	0.035	0.25	0.035
	$P_\downarrow$	$\bar{\Gamma}-\bar{M}$	0.24	0.070	0.24	0.098
		$\bar{\Gamma}-\bar{X}$	0.27	0.070	0.28	0.097
E_R (eV)	$P_\uparrow$	$\bar{\Gamma}-\bar{M}$	0.09	0.008	0.15	0.005
		$\bar{\Gamma}-\bar{X}$	0.11	0.008	0.16	0.005
	$P_\downarrow$	$\bar{\Gamma}-\bar{M}$	0.17	0.020	0.18	0.043
		$\bar{\Gamma}-\bar{X}$	0.19	0.020	0.20	0.040

orbit splitting. Thus, the mechanisms—or ingredients—for a considerable Rashba effect comprise (i) a strong atomic spin-orbit coupling, (ii) a steep surface-potential barrier, (iii) a strong in-plane potential gradient,[26] and (iv) a strong asymmetric charge density at the site of the heavy element (here: Bi) which can be induced by hybridization.

With respect to the latter one can speculate to control the Rashba splitting by an external electric field. An external electric field could cause a charge rearrangement in the topmost layers of a preferably highly polarizable substrate and, therefore, could affect the hybridization which—as outlined in this Brief Report—can result in a large spin splitting. This scenario calls for experimental and theoretical investigations.

ACKNOWLEDGMENT

This work is supported by the *Sonderforschungsbereich* 762 "Functionality of Oxide Interfaces."

*Corresponding author; samir@mpi-halle.de

[1] Y. A. Bychkov and E. I. Rashba, J. Phys. C **17**, 6039 (1984).
[2] S. Datta and B. Das, Appl. Phys. Lett. **56**, 665 (1990).
[3] N. Samarth, in *Solid State Physics*, edited by H. Ehrenreich and F. Spaepen (Elsevier, Amsterdam, 2004), Vol. 58, p. 1.
[4] I. Žutić, J. Fabian, and S. Das Sarma, Rev. Mod. Phys. **76**, 323 (2004).
[5] S. A. Wolf, A. Y. Chtchelkanova, and D. M. Treger, IBM J. Res. Dev. **50**, 101 (2006).
[6] J. Henk, M. Hoesch, J. Osterwalder, A. Ernst, and P. Bruno, J. Phys.: Condens. Matter **16**, 7581 (2004).
[7] M. Muntwiler, M. Hoesch, V. N. Petrov, M. Hengsberger, L. Patthey, M. Shi, M. Falub, T. Greber, and J. Osterwalder, J. Electron Spectrosc. Relat. Phenom. **137-140**, 119 (2004).
[8] C. R. Ast, J. Henk, A. Ernst, L. Moreschini, M. C. Falub, D. Pacilé, P. Bruno, K. Kern, and M. Grioni, Phys. Rev. Lett. **98**, 186807 (2007).
[9] F. Reinert, J. Phys.: Condens. Matter **15**, S693 (2003).
[10] L. Petersen and P. Hedegård, Surf. Sci. **459**, 49 (2000).
[11] Y. M. Koroteev, G. Bihlmayer, J. E. Gayone, E. V. Chulkov, S. Blügel, P. M. Echenique, and P. Hofmann, Phys. Rev. Lett. **93**, 046403 (2004).
[12] G. Bihlmayer, S. Blügel, and E. V. Chulkov, Phys. Rev. B **75**, 195414 (2007).
[13] L. Moreschini, A. Bendounan, I. Gierz, C. R. Ast, H. Mirhosseini, H. Höchst, K. Kern, J. Henk, A. Ernst, S. Ostanin, F. Reinert, and M. Grioni, Phys. Rev. B **79**, 075424 (2009).
[14] L. Moreschini, A. Bendounan, H. Bentmann, M. Assig, K. Kern, F. Reinert, J. Henk, C. R. Ast, and M. Grioni, Phys. Rev. B **80**, 035438 (2009).
[15] M. Nagano, A. Kodama, T. Shishidou, and T. Oguchi, J. Phys.: Condens. Matter **21**, 064239 (2009).
[16] H. Bentmann, F. Forster, G. Bihlmayer, E. V. Chulkov, L. Moreschini, M. Grioni, and F. Reinert, EPL **87**, 37003 (2009).
[17] H. Mirhosseini, I. V. Maznichenko, S. Abdelouahed, S. Ostanin, A. Ernst, I. Mertig, and J. Henk, Phys. Rev. B **81**, 073406 (2010).
[18] R. Winkler, *Spin-Orbit Coupling Effects in Two-Dimensional Electron and Hole Systems* (Springer, Berlin, 2003).
[19] S. Blügel and G. Bihlmayer, in *Computational Nanoscience: Do It Yourself!*, edited by J. Grotendorst, S. Blügel, and D. Marx (John von Neumann Institute for Computing, Jülich, 2006), Vol. 31, p. 85.
[20] Forschungszentrum Jülich, Institut für Festkörperforschung, Institute Quantum Theory of Materials, D-52425 Jülich, Germany.
[21] T. Toshio, K.-H. Hellwege, H. Landolt, R. Börnstein, and O. Madelung, in *Ferro- and Antiferroelectric Substances*, Landolt-Börnstein, New Series, Group III Vol. 3, edited by K.-H. Hellwege and A. M. Hellwege (Springer-Verlag, Berlin, 1981).
[22] M. Fechner, S. Ostanin, and I. Mertig, Phys. Rev. B **77**, 094112 (2008).
[23] M. Fechner, I. V. Maznichenko, S. Ostanin, A. Ernst, J. Henk, P. Bruno, and I. Mertig, Phys. Rev. B **78**, 212406 (2008b).
[24] *Electron Scattering in Solid Matter*, edited by J. Zabloudil, R. Hammerling, L. Szunyogh, and P. Weinberger (Springer, Berlin, 2005).
[25] J. Henk, in *Handbook of Thin Film Materials*, edited by H. S. Nalwa (Academic Press, San Diego, 2002), Vol. 2, Chap. 10, p. 479.
[26] J. Premper, M. Trautmann, J. Henk, and P. Bruno, Phys. Rev. B **76**, 073310 (2007).